



Dosimetry in the lungs of α -particles (^{210}Po) and β -particles (^{210}Pb) present in the tobacco smoke of conventional cigarettes and heated tobacco products

Laurent Desorgher^a, Aurélie Berthet^b, Jérémie Rossier^a, François Bochud^a,
Pascal Froidevaux^{a,*}

^a Institute of Radiation Physics, Lausanne University Hospital and University of Lausanne, Lausanne, Switzerland

^b University of Lausanne, Ctr Primary Care & Publ Hlth Unisanté, Lausanne, Switzerland

ARTICLE INFO

Keywords:

Polonium
Tobacco
Annual effective dose
Heat not burn
Dosimetry
Lung

ABSTRACT

Tobacco products contain radioactive ^{210}Pb and ^{210}Po which can be transferred from the filler to the mainstream smoke. When inhaled, they can contribute to the radioactive dose to the lungs and are suspected to significantly contribute to lung cancer from smoking. Currently, no data are available on the radioactive risk of the heated tobacco products (HTP). However, due to the relatively high heat involved in some of these devices, there are concerns about the volatility of polonium particles.

Here we used data on the ^{210}Po and ^{210}Pb content in tobacco smoke along with biokinetic and dosimetric models to compute the effective dose induced by conventional smoking and by using an HTP device (PMI IQOS system). Results show that conventional smoking of one pack per day induces a dose to the lung of about 0.3 mSv/year. This dose decreases by a factor of ten (0.03 mSv/year) for the IQOS system. However, this dose reduction is not obtained by specific countermeasures but by the fact that the IQOS system heats only 15% of the tobacco filler to the target temperature of 330 °C. When heated homogeneously to 300 °C, both conventional and Heets (IQOS) cigarettes release about 80% of the ^{210}Po from the tobacco, leading to similar doses to lungs.

1. Introduction

Natural polonium-210 (^{210}Po) and lead-210 (^{210}Pb) are present within and on the surface of tobacco leaves because the leaf trichomes capture radon-222 (^{222}Rn) progeny aerosols, with a smaller part originating from root transfer (Laking, 2019; Martell, 1974; Radford and Hunt, 1964; Skrable et al., 1964; Winters and Difranza, 1982). Aerosol particles of Pb and Po have significant volatility, which explains their presence in the mainstream of cigarette smoke. Energetic α -particle emitters are a potential carcinogenic component of lung cancer and contributed to the very high mortality rate from lung cancer found in several groups of underground mine workers exposed to radon progeny (Little and Otoole, 1974). In addition, as demonstrated in the case of the Colorado Plateau uranium miners, a high incidence of lung cancer was associated with the group of miners who were smoking cigarettes (Wagoner et al., 1963). Epidemiologic studies on the risk of lung cancer associated with residential ^{222}Rn exposure have confirmed the synergistic effect of combining cigarette smoking and exposure to

α -radiations, with efforts to reduce in-house ^{222}Rn very beneficial to smokers (Darby et al., 1998, 2005; Gray et al., 2009). As early as 1964, Radford and Hunt (1964) and Little et al. (1965, 1967, 1974) demonstrated the presence of ^{210}Po in tobacco smoke and its preferential localization in the bronchial epithelium of smokers, and hypothesized that it would be a cause of lung cancer. Little and O'Toole (1974) confirmed this hypothesis in Syrian golden hamsters, which showed increased lung epidermoid and adenocarcinomas after inhaling ^{210}Po particles. Despite these findings, the tobacco industry has made no successful effort to remove ^{210}Po and ^{210}Pb from tobacco (Laking, 2019; Muggli et al., 2008; Rego, 2009).

To measure the risk of damage caused by the radioactivity present in tobacco smoke, it is necessary to implement radiation dosimetry, which in turn makes it possible to compare with other radiation sources such as those used in medicine, or from occupational exposure or environmental exposure. The literature contains many studies investigating the annual dose to the lung caused by smoking (Boujelbane et al., 2020; Christobher et al., 2020; Duong et al., 2020; Ghanbar-Moghaddam and Fathivand,

* Corresponding author. Institute of Radiation Physics, Rue du Grand-Pré 1, CH-1007, Lausanne, Switzerland.

E-mail address: pascal.froidevaux@chuv.ch (P. Froidevaux).

2020; Kubalek et al., 2016; Mandic et al., 2016; Taroni et al., 2014; Tiwari et al., 2016). However, while the data on the ^{210}Po and ^{210}Pb content of tobacco is rather constant throughout these studies—about 15–25 mBq/cigarette—there is a large dispersion of the annual effective doses estimated from the cigarettes' content between studies. For a daily consumption of one pack per day (20 cigarettes), effective dose is as low as 30 μSv to as high as tens of mSv, depending on the scenario used for the transfer of radionuclides from the tobacco to the mainstream smoke, the particle size, the particle localization, the fraction deposited in the lung, and for the particle clearance rate. In fact, most of the studies recently published in this field simply use dose factors (mSv/Bq) estimated in previous studies and apply them to a basic inhalation scenario, thus leading to a strong divergence in dose estimation (Boujelbane et al., 2020; Christobher et al., 2020; Ghanbar-Moghaddam and Fathivand, 2020; Kubalek et al., 2016; Taroni et al., 2014). For instance, several studies used a transfer factor of 0.7–1.0 for the fraction of ^{210}Po in tobacco transferred to the mainstream smoke (Cankurt and Gorgun, 2020; Christobher et al., 2020), while several others, including this one, measured this fraction to be less than 0.15 (Schayer et al., 2010; Taki-zawa et al., 1994; Taroni et al., 2014). In addition, some studies calculated the annual dose for ^{210}Po only, while others calculated for the additional ^{210}Pb contribution. While some studies used a fast clearance rate for ^{210}Po particles, others used a slow clearance rate for both ^{210}Po and ^{210}Pb particles. Because of these divergences, we propose here a complete dosimetry of lung radiation exposure due to smoking. To do this, we measured, in a companion study, the ^{210}Po and ^{210}Pb content in the cigarette tobacco of 13 brands sold in Switzerland, including the heated tobacco product Heets (Philip Morris) (Berthet et al., 2022). In addition, we used a smoking machine to determine the particle size involved in the transfer of ^{210}Po and ^{210}Pb to the mainstream smoke and their transfer fraction to the mainstream smoke, for both conventional cigarettes and the heat-not-burn IQOS system (Berthet et al., 2022). Using these data, we implemented the recent ICRP intake models for ^{210}Po and ^{210}Pb in our dosimetry code with scenario of slow and moderate absorption into blood. Eventually, we estimated the annual effective dose induced by the smoking of one pack of cigarettes per day (i.e. 20 cigarettes) and a corresponding pack of heated tobacco product Heets (IQOS) (Bolch et al., 2016; Paquet et al., 2017).

2. Methods

2.1. Chemicals

Hydrogen peroxide solution (H_2O_2 35%), ascorbic acid, and NH_4FeSO_4 salts were purchased from Sigma-Aldrich (Switzerland) and were *puriss. p. a.* grade. Nitric acid solution (HNO_3 65%), hydrochloric acid solution (HCl 35%), and ammonia solution (NH_4OH 30%) were purchased from Carlo-Erba (Reactolab, Switzerland) and were analytical grade. Solutions (25 mBq/ml) of ^{208}Po and ^{209}Po were obtained from the Metrology group of the Institute of Radiation Physics, Lausanne and were traceable to NIST standard (^{209}Po , NIST SRM 4326) or NPL standard (^{208}Po , NPL A160443).

^{210}Po and ^{210}Pb in tobacco fillers and their transfer to mainstream smoke.

The data on ^{210}Po and ^{210}Pb in tobacco fillers and on ^{210}Po and ^{210}Pb transfer to the mainstream smoke for conventional smoking and IQOS/HTP smoking system were taken from a previous companion study available in open access, containing a full description of the methodology used (Berthet et al., 2022).

2.2. ^{210}Po particle size range determination

We used a smoking device designed in our facility to capture the mainstream aerosol and which was developed to meet the standards for tobacco cigarettes. The Health Canada Intense (HCI) regime was followed to generate smoke from conventional cigarettes and IQOS system

(version 2.4 and 3.0). Briefly, the cigarette (either conventional cigarette or Heet cigarette for IQOS) was connected to two filter holders containing a 0.8 μm and 0.22 μm acetate filters. The last filter holder was connected to three 250 ml washing flasks (F1–F3) containing 100 ml of 1M HCl each and linked in a series. The first filter holder was connected to the cigarette or IQOS Heet cigarette and the last washing flask (F3) was connected to the smoking machine. Eleven puffs of 55 ml for 2 s duration at a frequency of 30 s were programmed for each cigarette, including IQOS. The smoking was repeated on three cigarettes and the three 0.8 μm filters, the three 0.22 μm filters, and the three F1, F2 and F3 fractions were combined for increased sensitivity before ^{210}Po determination. Ashes and butts were combined similarly before ^{210}Po determination.

2.3. ^{210}Po determination

The filters (0.8 μm or 0.22 μm), the ashes, and the butts were weighed in a 100 ml Teflon flask and spiked with 25 mBq of ^{209}Po . Aliquots of 20 ml of concentrated HNO_3 (65%) and 3 ml of 30% H_2O_2 were added, and samples were digested in a pressurized microwave apparatus (Milestone UltraClave IV, Germany) under a pressure of 50 bars and at a temperature of 180 $^\circ\text{C}$ for 15 min. The solution was poured into a 300 ml beaker and diluted to 250 ml with ultrapure water. Two mg of Fe^{3+} were added and ^{210}Po was co-precipitated on iron hydroxides at pH 8 with addition of 30% NH_4OH . After decantation and centrifugation, the iron hydroxide precipitate was dissolved in 100 ml of 1M HCl and 1 g of ascorbic acid was added to reduce Fe^{3+} to Fe^{2+} . A silver disk (\varnothing 1 cm), covered on one face with tape, was suspended in the solution for 2 days, inducing the spontaneous electrochemical deposition of polonium isotopes on the disk. After retrieval, the disk was counted (400000–864000 s) on a surface barrier detector (PIPS) of 450 mm^2 in an Alpha Analyst Alpha Spectrometer (Canberra-Mirion, France). The combined F1, F2 and F3 fractions were treated as in Berthet et al. (2022) to determine ^{210}Po .

2.4. Dosimetry

The effective dose induced by the smoke of a cigarette was computed following the ICRP biokinetic and dosimetry models for the inhalation of ^{210}Pb and ^{210}Po (Bolch et al., 2016; Eckerman and Endo, 2008; Paquet et al., 2015, 2017). The activity of ^{210}Pb , ^{210}Po , and their progenitor in the human body organs over time was computed using the biokinetic model from ICRP 137 and ICRP 130 (Paquet et al., 2015, 2017). The equivalent dose from a source region where a radionuclide decay to a target region was computed by using specific absorbed fractions from ICRP 133 and radioactive decay data from ICRP 107 (Bolch et al., 2016; Eckerman and Endo, 2008). For a detailed description of the whole model we refer to ICRP publications (Bolch et al., 2016; Eckerman and Endo, 2008; Paquet et al., 2015, 2017). We describe here only the part of our model original to our study.

The committed effective dose received by the inhalation of 1 Bq of a radionuclide X (^{210}Pb or ^{210}Po) was computed by

$$E_{50}^{S,M}(X) = \sum_{C=E1,E2,BB,bb,Al} P(C) E_{50}^{S,M}(X, C) \quad (1)$$

where $E_{50}^{S,M}(X, C)$ represents the committed effective dose induced by the deposition of 1 Bq of radionuclide X in the compartment C of the respiratory tracts and the $P(C)$ coefficient represents the fraction of the inhaled isotopes that is deposited in the compartment. The same deposition model was considered for ^{210}Pb and ^{210}Po . The compartments of the respiratory tract considered for the deposition of the radionuclides were the extra-thoracic compartments ET1 and ET2, and the thoracic compartments bronchial (BB), bronchiolar (bb), and alveolar interstitial (AI). The superscripts S and M refer to the slow and moderate mode of absorption of the radionuclide from the respiratory tract into blood that

is recommended by the ICRP for computing effective dose for a smoker (Paquet et al., 2017).

The committed effective dose $E_{50}^{S,M}(X, C)$ was computed using our own implementation of the ICRP biokinetic and dosimetry models for the inhalation of ^{210}Pb and ^{210}Po . We considered the full decay chain of ^{210}Pb (with the contributions of ^{210}Bi and ^{210}Po). As a reminder, the ^{210}Po progeny (^{206}Pb) is stable. The initial deposition of the radionuclide in the respiratory tract was modeled following the study of Tiwari et al. (2016) on the distribution of particle sizes in tobacco smoke. The proportion of the inhaled radionuclide X that is initially deposited in compartment C was computed as

$$P(C) = \sum_{C_1} R(C_1, C) \int f(S) P_{\text{dep}}(S, C_1) dS \quad (2)$$

where $f(S)$ represents the distribution of the size S of the inhaled radionuclide particles taken as the averaged distribution measured by Tiwari et al. (2016) for ^{210}Po . In our model the same size distribution $f(S)$ is taken for ^{210}Pb and ^{210}Po . $P_{\text{dep}}(S, C_1)$ represents the proportion of particles initially deposited in the different parts of the respiratory tract C_1 considered in the model of Tiwari et al. (2016), namely the head airways ($C_1 = \text{HA}$), the trachea and bronchi ($C_1 = \text{TB}$), and the pulmonary system ($C_1 = \text{PU}$). $P_{\text{dep}}(S, C_1)$ was computed by Tiwari et al. (2016) with the Multiple-Path Particle Dosimetry (MPPD) model as a function of particle size. The coefficients $R(C_1, C)$ represent the proportion of particles deposited in C_1 that deposit in the compartment C of the respiratory tract of the ICRP biokinetic model (see Table 1). The values of $R(C_1, C)$ were selected to be close to the relative proportion of deposition in the different compartments C of the respiratory tract as used in the deposition model of the ICRP publication (Paquet et al., 2015).

Finally, the committed effective dose induced by smoking 1 cigarette was computed as

$$E_{50}^{S,M} = \sum_{X=^{210}\text{Pb}, ^{210}\text{Po}} A(X) F(X) E_{50}^{S,M}(X) \quad (3)$$

where $A(X)$ represents the measured activity of the radionuclide X contained in one cigarette and $F(X)$ the proportion of the radionuclide transferred from the cigarette to the smoke and inhaled by the smoker.

The parameters used in our dosimetry model to compute the committed effective dose are summarized in Table 1.

Table 1

Description of the parameters used in the dosimetry model and the values used in this study. Different ^{210}Po and ^{210}Pb contents are considered for conventional and IQOS cigarettes (cig.).

| Parameter | Value/reference | Remark |
|---|--|------------------------------------|
| ^{210}Po content of fillers $A(^{210}\text{Po})$ | 15.0 ± 2.3 mBq/cig. (conventional). 6.9 mBq/cig. (IQOS) | $A(^{210}\text{Po})$ in Equation 3 |
| ^{210}Pb content of fillers $A(^{210}\text{Pb})$ | 15.0 ± 3.3 mBq/cig. (conventional) 6.9 mBq/cig. (IQOS) | $A(^{210}\text{Pb})$ in Equation 3 |
| F (fraction of ^{210}Po transferred to the mainstream smoke) | $13.6 \pm 4.2\%$ (conventional cig.) 1.8% (IQOS cig.) | $F(^{210}\text{Po})$ in Equation 3 |
| F (fraction of ^{210}Pb transferred to the mainstream smoke) | $7.0 \pm 2\%$ (conventional cig.) 1.6% (IQOS cig.) | $F(^{210}\text{Pb})$ in Equation 3 |
| ^{210}Po and ^{210}Pb size distribution | Tiwari et al. (2016) | $f(S)$ in Equation 2 |
| $R(C_1, C)$ for head airways | $R(\text{HA}, \text{ET1}) = 0.65$ $R(\text{HA}, \text{ET2}) = 0.35$ | Equation 2 |
| $R(C_1, C)$ for trachea and bronchi | $R(\text{TB}, \text{BB}) = 1$ | Equation 2 |
| $R(C_1, C)$ for the pulmonary system | $R(\text{PU}, \text{bb}) = 0.2$ $R(\text{PU}, \text{AI}) = 0.8$ | Equation 2 |

3. Results

3.1. ^{210}Po and ^{210}Pb in cigarette filters and in the mainstream smoke

The activities of ^{210}Po and ^{210}Pb in cigarette filters and in the mainstream smoke were estimated and published in a previous study (Berthet et al., 2022). Briefly, the results of the analysis of 13 different cigarette brands gave a remarkably stable average value of 15.0 ± 2.3 mBq per cigarette or 25.2 ± 2.6 mBq.g⁻¹ tobacco ($n = 15$). IQOS Heets bronze label had an equivalent ^{210}Po content to conventional cigarettes (23.7 ± 2.1 mBq.g⁻¹ tobacco) but the filler contained about half the tobacco mass compared to a conventional cigarette (290 mg of tobacco compared to 600 mg for a conventional cigarette). We found also that the ^{210}Po activity is supported by a similar activity of ^{210}Pb ($^{210}\text{Po}/^{210}\text{Pb}$ ratio of 1.06 ± 0.05) in cigarettes sold in Switzerland. $13.6 \pm 4.2\%$ ($n=24$) of total ^{210}Po present in the cigarette was transferred to the mainstream smoke. This dropped to $1.8 \pm 0.3\%$ ($n = 8$) of the total ^{210}Po present in the Heets filler smoked with the IQOS system (Berthet et al., 2022). While ^{210}Pb and ^{210}Po were in secular equilibrium in the tobacco, it was not the case in the mainstream smoke and only $7 \pm 2\%$ of ^{210}Pb was transferred from the tobacco to the mainstream smoke in conventional cigarettes (1.6% for IQOS Heets). However, when the conventional cigarettes and Heets were heated at the target temperature of 330°C as postulated by the manufacturer (Philipp Morris) for IQOS, more than 80% of ^{210}Po was lost from the tobacco in both cases, demonstrating that only a small fraction of the tobacco is really heated at 330°C with IQOS. All these data form the core experimental results necessary to implement our dosimetry model to assess the dose to the lung based on the inhalation of ^{210}Po and ^{210}Pb particles for conventional and heated tobacco products.

3.2. ^{210}Po particle size range determination

Results showed that the filter of a conventional cigarette retained about 20% of the total ^{210}Po contained in the tobacco. This value dropped to 10% for IQOS Heets, showing that the IQOS Heets aerosol might be formed of smaller particles compared to conventional cigarettes. In conventional smoking, the $0.8\ \mu\text{m}$ filter retained 92% of the ^{210}Po present in the mainstream smoke, while 2.6% were found on the $0.22\ \mu\text{m}$ filter and about 5% passed into the combined three F1–F3 washing flasks. However, it was not possible to carry out this experiment with IQOS, because the aerosol, of a different nature (mostly glycerol) compared to conventional smoking, rapidly clogged the acetate filters. Tiwari et al. (2016) carried out a very interesting and complete study on the particle size of the mainstream smoke using a variable configuration cascade impactor (VCCI). Their results showed that the mass size distribution of mainstream cigarette smoke was comprised mostly of particles between $2\ \mu\text{m}$ and $0.1\ \mu\text{m}$ and that the ^{210}Po containing particles had the same distribution. Our coarse study based on filters confirmed the detailed analysis by Tiwari et al. (2016) with VCCI and we will therefore use their particle size distribution in this work because it is more complete. However, to our knowledge, no study yet exists of the particle size for the IQOS system. We therefore decided to use the same distribution as for conventional smoking, keeping in mind that the average particle size could be different.

3.3. Computed committed effective dose

Table 2 presents the computed committed effective dose induced by the deposition of 1 Bq in the different compartments of the respiratory tract. In order to validate our computation of the $E_{50}^{S,M}(X, C)$ presented in Table 2, we computed (Equation (1)) the effective dose obtained for the deposition models ($P(C)$) used by the ICRP for workers, and compared our results with the published values (Paquet et al., 2017). Data of both models are shown in Fig. 1.

Table 2

Computed committed effective dose induced by the deposition of 1 Bq of ^{210}Po and ^{210}Pb in the different compartments of the respiratory tracts. See term $E_{50}^{S,M}(X, C)$ in Equation (1).

| Respiratory tract compartments | slow absorption into blood E_{50}^S [Sv/Bq] | | moderate absorption into blood E_{50}^M [Sv/Bq] | |
|--------------------------------|---|-----------------------|---|-----------------------|
| | ^{210}Po | ^{210}Pb | ^{210}Po | ^{210}Pb |
| ET1 | 1.73×10^{-9} | 4.14×10^{-9} | 2.68×10^{-8} | 8.33×10^{-8} |
| ET2 | 1.46×10^{-6} | 6.75×10^{-6} | 6.91×10^{-7} | 6.38×10^{-7} |
| BB | 7.57×10^{-6} | 1.71×10^{-5} | 5.45×10^{-6} | 1.62×10^{-6} |
| bb | 3.64×10^{-5} | 5.73×10^{-6} | 2.93×10^{-5} | 1.30×10^{-6} |
| AI | 1.79×10^{-5} | 1.30×10^{-4} | 9.19×10^{-6} | 7.61×10^{-6} |

Table 3 presents the computed proportion of the inhaled radionuclides (P(C)) in Equations (2) and (3), which deposit in the different compartments of the respiratory tracts, compared with the one used in ICRP 130 for different particle sizes given in terms of activity median thermodynamic diameters (AMTD) and activity median aerodynamic diameters (AMAD) (Paquet et al., 2015). The values are presented in particular for an AMAD of $0.43 \mu\text{m}$ as the median diameter of the f(S) distribution measured by Tiwari et al. (2016) was $0.43 \mu\text{m}$. These values were obtained by interpolation of the values published in the ICRP 130 for AMAD = 0.3 and $0.5 \mu\text{m}$ (Paquet et al., 2015). The computed committed effective dose induced by the inhalation of 1 Bq of ^{210}Po and ^{210}Pb is shown in Table 4 and compared with the values obtained with the deposition model of ICRP 130 for different median particle diameters (Paquet et al., 2015). The results for AMTD = 0.01 and $0.1 \mu\text{m}$ were taken directly from the electronic annex of ICRP 137 (Paquet et al., 2017). The results for AMTD = $0.43 \mu\text{m}$ were computed with Equation (1) by considering the fraction deposited in the compartments of the respiratory tract as given in the last line of Table 3.

The computed committed effective dose induced per year by the smoke of 20 cigarettes per day is given in Table 5, for conventional smoking and IQOS. Both results are given for the slow and moderate mode of absorption from the respiratory tract to the blood. The low percentage of tobacco filler in Heets cigarette truly heated to 330°C is reflected in the corresponding low dose determination for IQOS, as only 1.8% of the ^{210}Po content of the filler is transferred to the mainstream smoke (Berthet et al., 2022).

Fig. 2 presents the yearly committed effective dose induced by the

smoke of 20 cigarettes per day computed with Equations (1)–(3), by using the deposition models proposed in ICRP 130 for workers, adults at rest, and active adults (Paquet et al., 2015). Results include both the case of slow (left) and of moderate (right) absorption in the blood, as a

Table 3

Computed fraction of the inhaled ^{210}Pb and ^{210}Po initially deposited in the different compartment of the respiratory tract (coefficient P(C) in Equations (2) and (3)). The values considered in ICRP 130 for different averaged size of the particles and for workers are also presented for comparison (Paquet et al., 2015).

| Aerosol deposition model | Fraction Deposited in the respiratory tract [% of inhaled Bq] | | | | |
|--|---|------|-------|-------|-------|
| | ET1 | ET2 | BB | bb | AI |
| This work (Tiwari distribution) | 2.23 | 1.2 | 12.86 | 5.12 | 20.47 |
| ICRP worker (AMTD = $0.01 \mu\text{m}$) | 12.06 | 6.5 | 3.01 | 18.91 | 47.17 |
| ICRP worker (AMTD = $0.1 \mu\text{m}$) | 4.17 | 2.25 | 0.73 | 4.707 | 20.73 |
| ICRP worker (AMAD = $0.43 \mu\text{m}$) | 10.84 | 5.84 | 0.75 | 2.51 | 13.1 |

Table 4

Computed committed effective dose induced by the inhalation of 1 Bq of ^{210}Po and ^{210}Pb as obtained in this work and compared to the values from ICRP 137 (Paquet et al., 2017).

| Aerosol deposition model | slow absorption into blood E_{50}^S [Sv/Bq] | | moderate absorption into blood E_{50}^M [Sv/Bq] | |
|---------------------------------------|---|-----------------------|---|-----------------------|
| | ^{210}Pb | ^{210}Po | ^{210}Pb | ^{210}Po |
| This work | 2.92×10^{-5} | 6.51×10^{-6} | 1.84×10^{-6} | 4.09×10^{-6} |
| ICRP worker AMTD = $0.01 \mu\text{m}$ | 6.5×10^{-5} | 1.6×10^{-5} | 3.8×10^{-6} | 1.0×10^{-5} |
| ICRP worker AMTD = $0.1 \mu\text{m}$ | 2.8×10^{-5} | 5.5×10^{-6} | 1.6×10^{-6} | 3.3×10^{-6} |
| ICRP worker AMAD = $0.43 \mu\text{m}$ | 1.77×10^{-5} | 3.4×10^{-6} | 1.09×10^{-6} | 2.03×10^{-6} |

Table 5

Computed committed effective dose per year induced by smoking 20 conventional cigarettes or 20 Heat-not-burn (Heets) cigarettes per day with IQOS.

| | slow absorption into blood E_{50}^S [mSv/year] | | | moderate absorption into blood E_{50}^M [mSv/year] | | |
|-------------------------|--|-------------------|-------|--|-------------------|-------|
| | ^{210}Pb | ^{210}Po | Total | ^{210}Pb | ^{210}Po | Total |
| Conventional cigarettes | 0.224 | 0.093 | 0.317 | 0.014 | 0.058 | 0.072 |
| Heets (IQOS) | 0.024 | 0.006 | 0.030 | 0.001 | 0.004 | 0.005 |

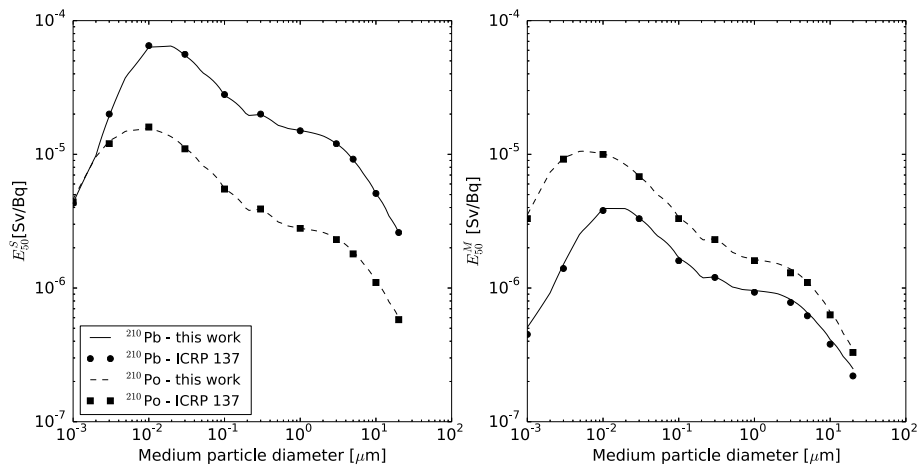


Fig. 1. Committed effective dose per inhaled activity of ^{210}Pb and ^{210}Po , for the cases of slow (left) and moderate (right) absorption into the blood, as computed with the present model and compared with values published in ICRP 137 for workers (Paquet et al., 2017). The results are presented as a function of the median particle diameter that represents the AMTD for diameters $<0.3 \mu\text{m}$ and the AMAD for diameters $>0.3 \mu\text{m}$.

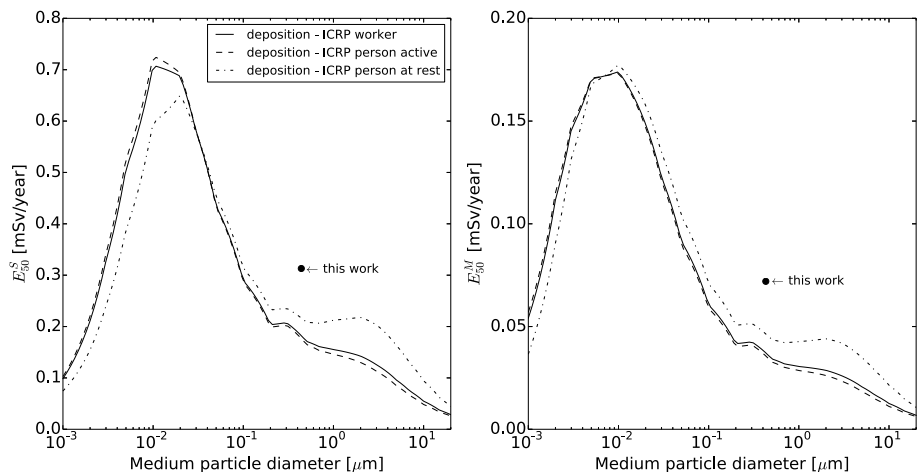


Fig. 2. Yearly committed effective dose induced by smoking 20 conventional cigarettes per day, computed with Equation (1) for different deposition models. Results include both the case of slow (left) and of moderate (right) absorption in the blood. See text for details.

function of the median diameters of the particles. The value obtained with the deposition model used in this work is indicated by a solid circle for a median diameter of 0.43 μm of the particle size distribution measured by Tiwari et al. (2016).

Table 6 compares the computed yearly committed effective dose induced by smoking a pack of 20 conventional cigarettes per day with the data from the literature. It is given for the case of slow absorption from the respiratory tract to the blood.

4. Discussion

To parameterize our model with sound data, especially for heated tobacco system (here IQOS) for which no data previously existed, we took data from a companion study in which we measured tobacco content in cigarettes sold in Switzerland, including Heets. Using a smoking machine, we then measured the transfer of ^{210}Po and ^{210}Pb in the mainstream smoke. For the IQOS system, we demonstrated that only 15% of the tobacco filler was really heated at the targeted 330 $^{\circ}\text{C}$ temperature (declared by the manufacturer), by using a radioactivity balance and by uniformly heating the tobacco in a cylindrical copper device (Berthet et al., 2022). This result is significant because it demonstrates that smoking with IQOS results in smoking less tobacco, but not protecting the smoker from ^{210}Po and ^{210}Pb by other means. Based on these previous results and tobacco mass in the filler that is about half the mass in a conventional cigarette, smoking one pack a day of Heets cigarettes

with IQOS results in “smoking” about 870 mg of tobacco (20×290×15%). This quantity becomes 9600 mg for a conventional smoker if we consider that in that case about 80% of the filler is smoked, thus about 10 times more. This outcome is reflected in the transfer of only 1.8% of the ^{210}Po from the filler to the mainstream smoke of IQOS, while the ^{210}Po transfer fraction is 14% in conventional smoking. This fact will obviously have a large impact on the computed effective dose to the lung for a smoker of a pack per day with IQOS, which decreases from 0.32 mSv/year (conventional cigarette) to only 0.03 mSv/year (see Table 6). However, this drastic drop in the effective dose of radiation when using IQOS only reflects the low percentage of tobacco heated to 330 $^{\circ}\text{C}$, and not the smoker habit.

In order to validate our computation of the $E_{50}^{S,M}(X, C)$ presented in Table 2, we computed (Equation (1)) the effective dose obtained for the deposition models ($P(C)$) used by the ICRP for workers, and compared our results with the published values (Paquet et al., 2017). Data from both models are shown in Fig. 1. Our model yielded results for the inhalation of ^{210}Po within 5% of the ICRP published values (Fig. 1, red square). The agreement was still better (2–3%) for the inhalation of ^{210}Pb with the mode of slow absorption into blood (black dot), but the differences increased up to 10% for the mode of moderate absorption into blood. It is worth mentioning that part of the differences, but not all, can be explained by the fact that the values published in the ICRP 137 are given with two significant figures while the values computed here are given with three significant figures.

Results presented in Table 3 show that the fraction deposited in the various compartments of the respiratory tract obtained with the deposition model presented in this work was close to the results using the deposition model proposed in ICRP 130 for a 0.1 μm median diameter of the particle (AMTD) (Paquet et al., 2015). However, larger differences were observed for the BB compartment, with our model calculating a significantly higher percentage of deposition (~13% of inhaled Bq). Significant differences were also observed when the AMAD in the ICRP deposition model was set to 0.43 μm , corresponding to the median diameter in the distribution $f(S)$ used in our model. The results presented in Table 4 confirm this as well, where the dose coefficient obtained in this work was close to the dose coefficient obtained by using the deposition model of the ICRP with an AMTD of 0.1 μm . However, the dose coefficient was significantly higher with our model compared to the ICRP result when the AMAD was set to 0.43 μm .

The results presented in Fig. 2 confirm that the computed dose depends significantly on the deposition model, which is itself strongly influenced by the size of the particles, as can be seen for our computed value (single black circle), which was significantly larger than those of the ICRP model with a similar median particle diameter. On the other

Table 6
Computed yearly committed effective dose [mSv/year] due to ^{210}Po and ^{210}Pb , induced by the smoking of 20 conventional cigarettes per day for this study alongside data from several other studies. The dose conversion coefficients that can be used to compute the committed effective dose from the inhaled activity are given in column 3, where available.

| Reference | Inhaled activity [mBq/cig] | | Dose Conversion Coefficient [$\mu\text{Sv/Bq}$] | | Effective Dose [mSv/year] |
|----------------------------|----------------------------|-------------------|---|-------------------|---------------------------|
| | ^{210}Po | ^{210}Pb | ^{210}Po | ^{210}Pb | |
| This work | 1.95 | 1.05 | 6.5 | 29.2 | 0.32 |
| Tiwari et al. (2016) | | | 4.3 | 5.6 | 0.30 |
| Khater (2004) | 6.15 | | 4.3 | 5.6 | 0.44 |
| Skwarzec et al. (2001) | 4.8 | 4.8 | 1 | 2 | 0.11 |
| Iwaoka and Yonehara (2012) | | | | | 0.27 |
| Christobher et al. (2020) | | | | | 0.15 |
| Mandic et al. (2016) | | | | | 0.77 |

hand, the differences between the results of the ICRP model for the active adult, the adult at rest and the worker were small. However, the committed effective dose computed with our deposition model was conservative resulting in a higher dose compared to the value computed with the ICRP 130 deposition model, if the median diameter of the particles was higher than $0.1\ \mu\text{m}$ (Paquet et al., 2015).

Our dose computation did consider the ^{210}Bi contribution to the dose, in terms of it as the progeny of the inhaled ^{210}Pb , however, we did not consider the contribution of the inhalation of the ^{210}Bi contained in the cigarette. As the effective dose coefficients for the inhalation of 1 Bq of ^{210}Bi is 1–2 orders of magnitude smaller than those for ^{210}Po and ^{210}Pb , this contribution can be neglected.

Finally, Table 6 compares the computed yearly committed effective dose induced by smoking a pack of 20 conventional cigarettes per day with the data from the literature. We present here the highest computed effective dose obtained for the mode of slow absorption as most previous studies also considered a slow absorption from the respiratory tract to blood. This represents the most conservative case in which the inhaled particles will mostly stay in the respiratory tract and induce a significant dose by alpha and electrons into the lungs. The committed effective dose values are within the range of 0.1–0.8 mSv/year. The differences in the dose values reflect the differences of inhaled activity considered in the range of studies and various dose coefficients used in those studies. Our value of 0.32 mSv/year is well between the extreme values and close to most reported ones.

5. Conclusions

In this study, we present a detailed computation of the dose induced by the smoking of cigarettes based on the ICRP biokinetic and dosimetry models for the inhalation of ^{210}Pb and ^{210}Po . Our work is original in several aspects. First, we determined in a previous paper the average activity of 13 cigarette brands sold in Switzerland, including the Heets cigarette used in the heated tobacco IQOS system. We also used a smoking machine and a standardised smoking regime (HCI) to determine the fraction of ^{210}Po and ^{210}Pb transferred to the mainstream smoke (Berthet et al., 2022). Then, contrary to most previous studies on the ^{210}Po dosimetry to the lung caused by smoking which used conversion coefficients to compute the committed effective dose from the inhaled activity, we used a specific model of the deposition of the inhaled particles in the respiratory tract. This model is based on the particle size distribution published by Tiwari et al. (2016), who used a complete set of variable configuration cascade impactor (VCCI) to determine the polonium particles' size fractionation. Our full model resulted in a committed effective dose of 0.32 mSv/year, induced by the smoking of 20 conventional cigarettes per day. We added to these calculations the determination of the dose induced by the smoking of 20 Heets cigarettes smoked with the IQOS system. In that particular case, we found that the committed effective dose was roughly 10 times lower than for conventional cigarettes. The reason for this drastic drop was that IQOS heats only a small fraction (~15%) of the tobacco filler in a Heets cigarette to the targeted $330\ ^\circ\text{C}$ temperature, resulting in the transfer of only 1.8% of the ^{210}Po in the tobacco smoke. Note, however, this does not mean that IQOS smoking is less dangerous than conventional smoking in terms of radiation risk because our results do not involve the smoker's habit. It is possible that since an IQOS smoker "smokes" much less tobacco with the IQOS system compared to conventional smoking, their requirement may not be totally fulfilled, thus increasing the need to smoke more Heets cigarettes.

The committed effective dose computed with our model is close to the one obtained with the dose coefficients published in ICRP 137 for workers with inhaled particles of an activity median thermodynamic diameter (AMTD) of $0.1\ \mu\text{m}$ (Paquet et al., 2017). In this study, we show how the computed committed dose highly depends on the deposition model used and on the median size of the particles, confirming the importance of precisely measuring the particle size distribution in

cigarette smoke.

While the dose coefficients for the inhalation of radioactive particles proposed by the ICRP have been reviewed several times and appear to be currently consensual (Bolch et al., 2016; Paquet et al., 2015, 2017), the principal drawback of using them to estimate dose from cigarette smoking is the lack of experimental data on the localization of the deposition of ^{210}Pb and ^{210}Po particles along the respiratory track and in the lungs. To our knowledge, there exist only two previous studies Little et al. (1965), 1967 that determined the localization of the radioactive deposit by measuring the ^{210}Po in different compartments of the trachea and lungs of deceased smokers. They date back to the 1960s and showed that the radioactive deposit occurred in hot spots, leading to high doses at specific locations (bronchial bifurcations). Because at that time the use of a filter with cigarettes was not the norm, we can expect that the particle size and deposition along the respiratory track and lungs might be significantly different now. Thus, there is room for new studies of ^{210}Po and ^{210}Pb deposition in the lungs to increase the accuracy of the dosimetric model. This is particularly true in view of the calculated doses (see Table 6), which under specific parameters lead to values approaching the annual dose limit to the public of 1 mSv. If reached, most national regulations would impose an associated health warning pictogram or even the radioactive logo on cigarette packs (Swayampakala et al., 2015).

Funding

The study was funded by the Swiss Federal Office of Public Health (PF, contract n°18.010124/434.0000–204/1).

Declaration of competing interest

The authors declare the following financial interests/personal relationships which may be considered as potential competing interests: Pascal Froidevaux reports financial support was provided by Swiss Federal Office of Public Health.

Data availability

Data will be made available on request.

Acknowledgments

The Swiss Federal Office of Public Health is thanked for its support. F. Barraud is thanked for her help in ^{210}Po measurements.

References

- Berthet, A., Butty, A., Rossier, J., Sadowski, I.J., Froidevaux, P., 2022. (^{210}Po and (^{210}Pb content in the smoke of heated tobacco products versus conventional cigarette smoking. *Sci. Rep.* 12, 10314 <https://doi.org/10.1038/s41598-022-14200-2>.
- Bolch, W.E., Jokisch, D., Zankl, M., Eckerman, K.F., Fell, T., Manger, R., Endo, A., Hunt, J., Kim, K.P., Petoussi-Hens, N., 2016. ICRP Publication 133: the ICRP computational framework for internal dose assessment for reference adults: specific absorbed fractions. *Ann. ICRP* 45, 5–73. <https://doi.org/10.1177/0146645316661077>.
- Boujelbane, F., Samaali, M., Rahali, S., Dridi, W., Abdelli, W., Oueslati, M., Takriti, S., 2020. The activities of Po-210 and Pb-210 in cigarette smoked in Tunisia. *Radiat. Environ. Biophys.* 59, 565–570. <https://doi.org/10.1007/s00411-020-00853-y>.
- Cankurt, S., Gorgun, A.U., 2020. Determination and distribution of Po-210 in different morphological parts of tobacco plants and radiation dose assessment from cigarettes in Turkey. *Ecotoxicol. Environ. Saf.* 197, 110603 <https://doi.org/10.1016/j.ecoenv.2020.110603>.
- Christobher, S., Periyasamy, M., Athif, P., Mohamed, H.E.S., Bukhari, A.S., Hameed, P.S., 2020. Activity concentration of polonium-210 and lead-210 in tobacco products and annual committed effective dose to tobacco users in Tiruchirappalli District (Tamil Nadu, India). *J. Radioanal. Nucl. Ch.* 323, 1425–1429. <https://doi.org/10.1007/s10967-019-06879-x>.
- Darby, S., Hill, D., Auvinen, A., Barrios-Dios, J.M., Baysson, H., Bochicchio, F., Deo, H., Falk, R., Forastiere, F., Hakama, M., Heid, I., Kreienbrock, L., Kreuzer, M., Lagarde, F., Makelainen, I., Muirhead, C., Oberaigner, W., Pershagen, G., Ruano-Ravina, A., Ruosteenoja, E., Rosario, A.S., Tirmarche, M., Tomasek, L., Whitley, E., Wichmann, H.E., Doll, R., 2005. Radon in homes and risk of lung cancer:

- collaborative analysis of individual data from 13 European case-control studies. *Br. Med. J.* 330, 223–226. <https://doi.org/10.1136/bmj.38308.477650.63>.
- Darby, S., Whitley, E., Silcocks, P., Thakrar, B., Green, M., Lomas, P., Miles, J., Reeves, G., Fearn, T., Doll, R., 1998. Risk of lung cancer associated with residential radon exposure in south-west England: a case-control study. *Br. J. Cancer* 78, 394–408. <https://doi.org/10.1038/bjc.1998.506>.
- Duong, H.V., Nguyen, D.T., Peka, A., Toth-Bodrogi, E., Kovacs, T., 2020. Po-210 in soil and tobacco leaves in Quang Xuong, Vietnam and estimation of annual effective dose to smokers. *Radiat. Protect. Dosim.* 192, 106–112. <https://doi.org/10.1093/rpd/ncaa181>.
- Eckerman, K., Endo, A., 2008. ICRP Publication 107. Nuclear decay data for dosimetric calculations. *Ann. ICRP* 38, 7–96. <https://doi.org/10.1016/j.icrp.2008.10.004>.
- Ghanbar-Moghaddam, B., Fathivand, A., 2020. Study of Polonium-210 in Persian cigarettes and tobacco crops. *Radiat. Protect. Dosim.* 191, 335–340. <https://doi.org/10.1093/rpd/ncaa130>.
- Gray, A., Read, S., McGale, P., Darby, S., 2009. Lung cancer deaths from indoor radon and the cost effectiveness and potential of policies to reduce them. *Br. Med. J.* 338, a3110. <https://doi.org/10.1136/bmj.a3110>.
- Iwaoka, K., Yonehara, H., 2012. Natural radioactive nuclides in cigarettes and dose estimation for smokers. *J. Radioanal. Nucl. Chem.* 293, 973–977. <https://doi.org/10.1007/s10967-012-1808-9>.
- Khater, A.E.M., 2004. Polonium-210 budget in cigarettes. *J. Environ. Radioact.* 71, 33–41. [https://doi.org/10.1016/s0265-931x\(03\)00118-8](https://doi.org/10.1016/s0265-931x(03)00118-8).
- Kubalek, D., Sersa, G., Strok, M., Benedik, L., Jeran, Z., 2016. Radioactivity of cigarettes and the importance of Po-210 and thorium isotopes for radiation dose assessment due to smoking. *J. Environ. Radioact.* 155, 97–104. <https://doi.org/10.1016/j.jenvrad.2016.02.015>.
- Laking, G.R., 2019. Human exposure to radioactivity from tobacco smoke: systematic review. *Nicotine Tob. Res.* 21, 1172–1180. <https://doi.org/10.1093/ntr/nty111>.
- Little, J.B., Otoole, W.F., 1974. Respiratory-tract tumors in hamsters induced by benzo(a)pyrene and Po-210 alpha-radiation. *Cancer Res.* 34, 3026–3039.
- Little, J.B., Radford, E.P., Holtzman, R.B., 1967. Polonium-210 in bronchial epithelium of cigarette smokers. *Science* 155, 606–607. <https://doi.org/10.1126/science.155.3762.606>.
- Little, J.B., Radford, E.P., McCombs, H.L., Hunt, V.R., 1965. Distribution of Polonium-210 in pulmonary tissues of cigarette smokers. *N. Engl. J. Med.* 273, 1343–1351. <https://doi.org/10.1056/nejm196512162732501>.
- Mandic, L.J., Dolic, M., Markovic, D., Todorovic, D., Onjia, A., Dragovic, S., 2016. Natural radionuclides in cigarette tobacco from Serbian market and effective dose estimate from smoke inhalation. *Radiat. Protect. Dosim.* 168, 111–115. <https://doi.org/10.1093/rpd/ncv010>.
- Martell, E.A., 1974. Radioactivity of tobacco trichomes and insoluble cigarette-smoke particles. *Nature* 249, 215–217. <https://doi.org/10.1038/249215a0>.
- Muggli, M.E., Ebbert, J.O., Robertson, C., Hurt, R.D., 2008. Waking a sleeping giant: the tobacco industry's response to the polonium-210 issue. *Am. J. Publ. Health* 98, 1643–1650. <https://doi.org/10.2105/ajph.2007.130963>.
- Paquet, F., Bailey, M.R., Leggett, R.W., Lipsztein, J., Marsh, J., Fell, T.P., Smith, T., Nosske, D., Eckerman, K.F., Berkovski, V., Blanchardon, E., Gregoratto, D., Harrison, J.D., 2017. ICRP publication 137: occupational intakes of radionuclides: Part 3. *Ann. ICRP* 46, 1–486. <https://doi.org/10.1177/0146645317734963>.
- Paquet, F., Etherington, G., Bailey, M.R., Leggett, R.W., Lipsztein, J., Bolch, W., Eckerman, K.F., Harrison, J.D., 2015. ICRP publication 130: occupational intakes of radionuclides: Part 1. *Ann. ICRP* 44, 5–188. <https://doi.org/10.1177/0146645315577539>.
- Radford, E.P., Hunt, V.R., 1964. Polonium-210 – volatile radioelement in cigarette. *Science* 143, 247–249. <https://doi.org/10.1126/science.143.3603.247>.
- Rego, B., 2009. The polonium brief A hidden history of cancer, radiation, and the tobacco industry. *Isis* 100, 453–484. <https://doi.org/10.1086/644613>.
- Schayer, S.R., Qu, Q.S., Wang, Y.L., Cohen, B.S., 2010. Pb-210: a predictive biomarker of retrospective cigarette smoke exposure. *Cancer Epidemiol. Biomarkers* 19, 338–350. <https://doi.org/10.1158/1055-9965.epi-09-1008>.
- Skraale, K.W., Haughey, F.J., Little, J.B., Hunt, V.R., Radford, E.P., Alexander, E.L., 1964. Polonium-210 in cigarette smokers. *Science* 146, 86. <https://doi.org/10.1126/science.146.3640.86>.
- Skwarzec, B., Ulatowski, J., Struminska, D.I., Borylo, A., 2001. Inhalation of Po-210 and Pb-210 from cigarette smoking in Poland. *J. Environ. Radioact.* 57, 221–230. [https://doi.org/10.1016/s0265-931x\(01\)00018-2](https://doi.org/10.1016/s0265-931x(01)00018-2).
- Swayampakala, K., Thrasher, J.F., Hammond, D., Yong, H.H., Bansal-Travers, M., Krugman, D., Brown, A., Borland, R., Hardin, J., 2015. Pictorial health warning label content and smokers' understanding of smoking-related risks—a cross-country comparison. *Health Educ. Res.* 30, 35–45. <https://doi.org/10.1093/her/cyu022>.
- Takizawa, Y., Zhang, L., Zhao, L., 1994. Pb-210 and Po-210 in tobacco with a special focus on estimating the doses of Po-210 to man. *J. Radioanal. Nucl. Chem.* 182, 119–125. <https://doi.org/10.1007/bf02047974>.
- Taroni, M., Zaga, V., Bartolomei, P., Gattavecchia, E., Pacifici, R., Zuccaro, P., Esposito, M., 2014. Pb-210 and Po-210 concentrations in Italian cigarettes and effective dose evaluation. *Health Phys.* 107, 195–199. <https://doi.org/10.1097/hp.000000000000104>.
- Tiwari, M., Sahu, S.K., Bhargare, R.C., Pandit, G.G., 2016. Polonium in size fractionated mainstream cigarette smoke, predicted deposition and associated internal radiation dose. *J. Environ. Radioact.* 162, 251–257. <https://doi.org/10.1016/j.jenvrad.2016.06.005>.
- Wagoner, J.K., Haij, M.E., Miller, R.W., Fraumeni, J.F., Lundin, F.E., 1963. Unusual Cancer mortality among a group of underground metal miners. *N. Engl. J. Med.* 269, 284–289. <https://doi.org/10.1056/nejm196308082690602>.
- Winters, T.H., Difranza, J.R., 1982. Radioactivity in cigarette-smoke. *N. Engl. J. Med.* 306, 364–365.